EasyChair Preprint

№ 8767

Changes in the Gamma Spectra of Radioactive Materials Affected by Altering Neutrino Flux

Itzhak Orion

August 30, 2022

Changes in the Gamma Spectra of Radioactive Materials Affected by Altering Neutrino Flux

Itzhak Orion

Abstract

Neutrinos are particles with miniscule mass, and scholars consider their detection very challenging on account of their transparency. However, in previous studies we demonstrated that changes in neutrino flux affect the gamma count rates of various radioactive nuclei. Alterations in the emitted gamma energy spectra were measured following an increase in the neutrino flux. The manner in which the spectrum is affected may hint at the mechanism via which the neutrino interacts with the radio-nucleus. The spectra for Thorium, Ba-133, Mn-54, and Cs-137 were measured using an NaI(Tl) spectrometer. Two cyclotrons with 18 MeV proton beams were operated simultaneously, thus increasing the neutrino flux. The study found that the intensity of the spectra dropped in all four specimens following an increase in neutrino flux. The photofraction ratio remained unchanged in the decreased events. The photopeak analysis for mono-energetic gamma radiation nuclides revealed anomalies. This implies that the neutrino interacts with radio-nuclei by altering the gamma transition multipolarity, suggesting that neutrinos might interact with the nucleus in ways not considered by the present theory of nuclear physics.

Keywords: Radio-nuclei, Gamma, NaI(Tl), Neutrino

Introduction

In recent years, scholars have devoted growing attention to detecting neutrinos, which is known to be a complicated task. The detection method utilizes a large scale detector located deep underground or distant from radiation interference, which can affect detection ability[1-14]. Most of the detectors developed in recent years operate similarly to the thinking patterns developed by Raymond Davis, who established a large detector located deep underground[15]. Studies recently sought to detect neutrinos during solar flares (when the neutrino flux increases by three to four orders of magnitude[16]) using the following radioactive materials: Am-241, Rn-222, Thorium, Mn-54, and Co-57[17-20]. A decrease in the gamma count rate was detected in all the tested nuclei following the occurrence of solar flares. Studies found that each tested radioactive source exhibits a different decrease in gamma radiation counts. All measurements were conducted using an NaI(Tl) gamma ray detector set in a total-counts mode.

To confirm that neutrinos can interact with radionuclides, the radioactive sources were placed in front of a controlled neutrino source, a medical proton cyclotron. Neutrino flux during cyclotron operation was found to affect the decay rates of several radionuclides: for Am-241, there was a delay of 14 days between cyclotron operation and the decrease in the gamma count rate; for Rn-222 and its progeny, there was a delay of several hours between the cyclotron operation and the decrease in the gamma count rate; there was a delay of nine days for Thorium with its progeny, and for Co-57 a delay of about six days was recorded[21].

Detection inadequacy can occur when using an NaI(Tl) scintillator to measure gamma radiation. The simplest way to pinpoint malfunctions in the detector is to perform continuous spectral measurements. It is important to note that the NaI(Tl) detector is sensitive to extreme temperature changes; therefore, it is crucial that temperature stability be monitored[22]. Another type of problem relates to the electronics of the detector. In this case, the noise-to-signal ratio will increase, and, consequently, variations in the fluctuations will be observed in the counts. Electronic faults can also be detected in non-spectral NaI(Tl) detectors (single channel detectors).

If the detector works properly, repeatability of the measurements is maintained. One type of common problem in NaI(Tl) detectors relates to crystals, resulting in a broadening of the peaks due to instabilities of high voltage bias.

NaI(Tl) detection problems can be discerned by repeating spectral measurements to confirm that the results obtained are appropriate and the detector is not beset by the difficulties mentioned above. In addition, spectral repetition indicates that bias voltage is stable.
In the following experiments, the spectral measurements were repeated every 15 minutes. This ensures that the detector is working at the desired level of performance.
The aim of this study is to continue our previous study that dealt with a method for measuring changes in count rates of gamma radiation from radioactive nuclei caused by varying fluxes of neutrinos emitted by cyclotrons. We utilized an NaI(Tl) gamma radiation spectrometer that was enclosed with a Multi Chanel Analyzer (MCA) to ensure detection quality and to determine in which part of the gamma radiation spectrum the change takes place.

Our previous research established

Methods

A radiation spectrometry measurement system of NaI(Tl) detectors (3" diameter by 3" length) was installed facing the following radioactive sources: Thorium, Mn-54, Ba-133, and Cs-137. The detector was shielded by 5 cm thick lead. Data was collected every 15 minutes by the MCA, which can distinguish between the different energies of gamma radiation that reach the detector. MCA scintiSPEC (FLIR Systems, Inc.) was used to supply voltage and amplifier-gain to the detector. The results for each spectrum were totaled to obtain total counts and thus rapidly analyze whether a change occurs in the NaI(Tl) response. The detector energy calibration was preformed using a Cs-137 point source and a K-40 source (KCl salt), similarly to our previous studies[23].

Each dip in the total counts was compared to a baseline taken around the dip. Based on this we averaged a bundle of spectra, channel by channel, during the dip, and the same number of spectra from the baseline were also averaged[24]. A ratio function vs channel number, R(ch), was calculated for the averaged spectra as follows:

$$R(ch) = \frac{\langle Baseline(ch)\rangle - \langle dip(ch)\rangle}{\langle Baseline(ch)\rangle + 1} \quad (1)$$

Occasionally, the count in certain channels in a spectrum is zero. Therefore, we added 1 to the baseline values in the denominator.

The representation of R(ch) versus channel-number gives peaks at which the baseline counts are larger than the dip counts and dips at which the counts are larger than the baseline counts.

To analyze the decrease in the spectrum results, we defined each photopeak centroid channel number and its FWHM (full width half maximum) to signify the region of interest (ROI). The R(ch) ratios in the ROIs were averaged[25].

Previous studies have demonstrated that a proton accelerator can be used as a neutrino source[26-28]. Therefore, this study employed a proton accelerator, a medical proton cyclotron (as in our previous study): the two cyclotrons that were used together produce about $2.5 \cdot 10^8$ neutrinos in a quarter of an hour[21]. The two cyclotrons are located at around 20 m and 40 m from the measurement system.

Results and Discussion

Measurements for four radioisotope spectra were recorded using the NaI(Tl) detector: Thorium, Ba-133, Mn-54, and Cs-137. Each measurement system consists of an NaI(Tl) detector facing one of the radioisotopes. The NaI(Tl) detector was operated in MCA mode (1024 channels counting mode) for 15 min cycles, and total counts for each spectrum were recorded in order to discern decreases in the spectrum due to neutrino flux emitted from the two cyclotrons. The count decrease results were obtained following the operation of the two cyclotrons.

Thorium system

Measurements for a natural Thorium source with activity of about 15 μCi were recorded throughout a 36-day period using a detector connected to an MCA. First, the measurements were performed with a natural thorium using the spectral system. The thorium source obtained decreases using the total counts, as in our previous measurements[21]. Hence, the results verify our previous measurements.

The spectral data were collected at intervals of 15 minutes. All the counts, channel-by-channel, were summed into a total-counts value. When both cyclotrons were operated simultaneously, decreases in the total count rate were observed, as shown, for example, in Fig.1. Five decreases in the total counts were observed in the thorium source counts. The decreases and cyclotron operation details are summarized in Table 1.

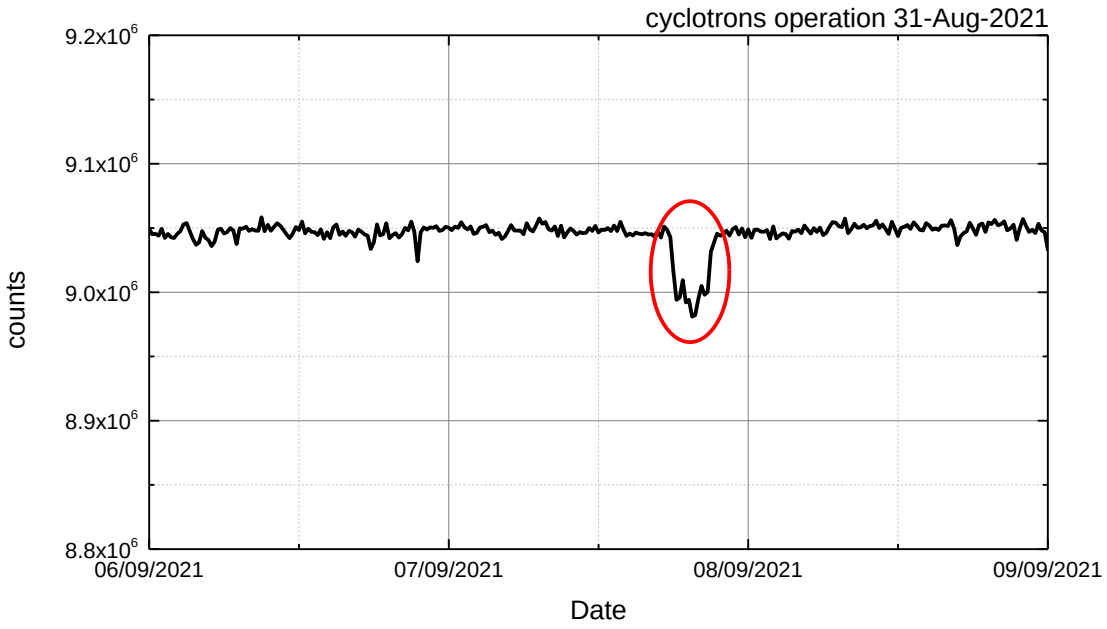

Figure 1- The total count mode of Thorium. The red circle marks a dip resulting from interactions with neutrinos emitted by two cyclotrons operating simultaneously.

The spectrum scored during a dip was analyzed using the following formula to calculate the percentage of the decrease:

$$Count\ decrease\ (\%) = \frac{\langle baseline \rangle - \langle dip \rangle}{\langle baseline \rangle} \cdot 100\%$$

Where the baseline is the average of the total-counts value, when no decreases were observed, and the dip is the decrease in total counts.

Table 1- Summary of the total counts for Thorium system responses following dual cyclotron operation.

Date of cyclotron operation	cyclotron	Duration (hr)	Current (μA)	Date of sharp dip	Delay (days)	Count decrease (%)
04-Aug-2021	1	2:20	73	10-Aug-2021	7	-0.44%
	2	3:10	73			
17-Aug-2021	1	3:15	74	24-Aug-2021	8	-0.62%
	2	2:50	75			
23-Aug-2021	1	2:00	74	30-Aug-2021	8	-0.34%
	2	3:00	74			
26-Aug-2021	1	3:15	75	31-Aug-2021	5	-0.68%
	2	3:40	75			
31-Aug-2021	1	4:30	74	07-Sep-2021	8	-0.54%
	2	6:20	74			

Signal detectability verification and the reliability of the Thorium system results were performed using the 'limits-of-detectability' method[22]. The critical level (LC) was calculated using the neighboring counts. Subsequently, dip counts were compared to the LC. Once the presented dip counts exceeded the LC value, the dip detection is reliable.

$$\%L_C = \frac{Neighboring\ Counts - Lc}{Neighboring\ Counts} \cdot 100\% = 0.12\%.$$

Therefore, all five decreases in the total count, as presented in Table 1, are considered statistically significant. However, when comparing a spectrum at the dip to a spectrum at the neighboring baseline, the changes are barely noticeable; indeed, the observed decreases are less than one percent of the total count. Dividing the counts into 1024 channels in the MCA process made the statistical confidence in each channel low.

The spectrum shown in Fig.2A is an average of the 12 spectra for which decreases were obtained. Fig.2A is a graphical comparison of the dip spectra and the baseline spectra; the change in the spectra could not be clearly distinguished. Fig.2B shows the analyzed spectra according to the R(ch) function (Eq.1). Fig.2 is a sample graph of the spectral analysis decrease received on September 7, 2021; the counts in the NaI(Tl) detector are statistically significant up to an energy of about 1000 keV. Therefore, we present the graph up to 1000 keV only, although the obtained readings are up to 3000 keV. In Fig.2B the ratio R(ch) indicates that the entire spectrum alters between dip counts and baseline counts.

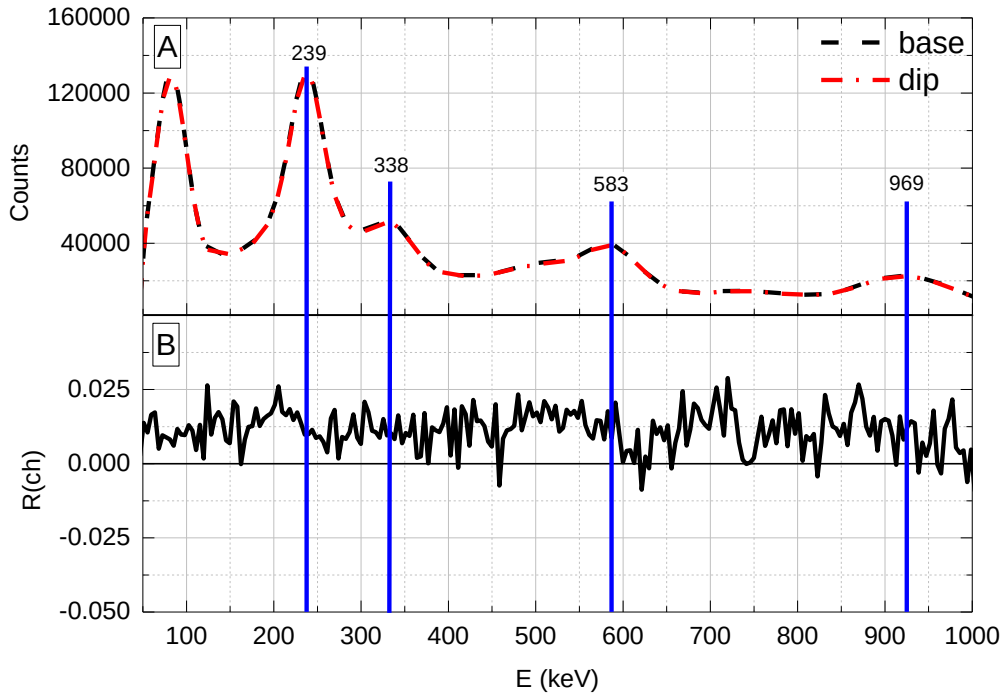

Figure 2- A) The spectrum obtained for Thorium after averaging 12 spectra at the time when the dip occurred (dashed red line) and after averaging 12 spectra of the baseline before the dip occurred (black dashed line). B) is the ratio change R(ch) calculated for these spectra. The blue vertical lines show the gamma energy emission lines of Thorium and its progeny.

R(ch) function for each dip spectra was performed, and a decrease in the total total-counts was observed.

NaI(Tl) spectrometry has a moderate spectral resolution; therefore, it is recommended that the peak counts along the range of channels in which the peak is detected should be analyzed.

Around each photopeak of Thorium, an ROI range was set, and for each ROI range, the R(ch) ratios were totaled over its channels, as presented in Table 2.

Table 2- Summary of the ROI in the R(ch) of the five dips in table 1, where each channel is 4.29 keV

Date:			10-Aug-21	24-Aug-21	30-Aug-21	31-Aug-21	07-Sep-21
E (keV)	Peak Ch	ROI Ch	Ratio Sum				
239	55	47-63	0.084	0.067	0.109	0.219	0.092
338	76	70-90	0.103	0.076	0.150	0.227	0.089
583	136	116-149	0.142	0.117	0.228	0.393	0.181
969	216	192-234	0.200	0.160	0.328	0.411	0.224
1573	367	324-399	0.394	0.275	0.473	0.905	0.248
2105	491	452-551	0.536	0.450	0.736	0.776	0.712
2620	599	577-626	0.175	0.197	0.554	0.346	0.338

Table 2 suggests that in all the ROI a positive number was found. i.e., the decreases obtained in the total counts were indicated in all the photopeaks along the spectrum. Compton scattering, at lower energies, likewise demonstrated the decrease.

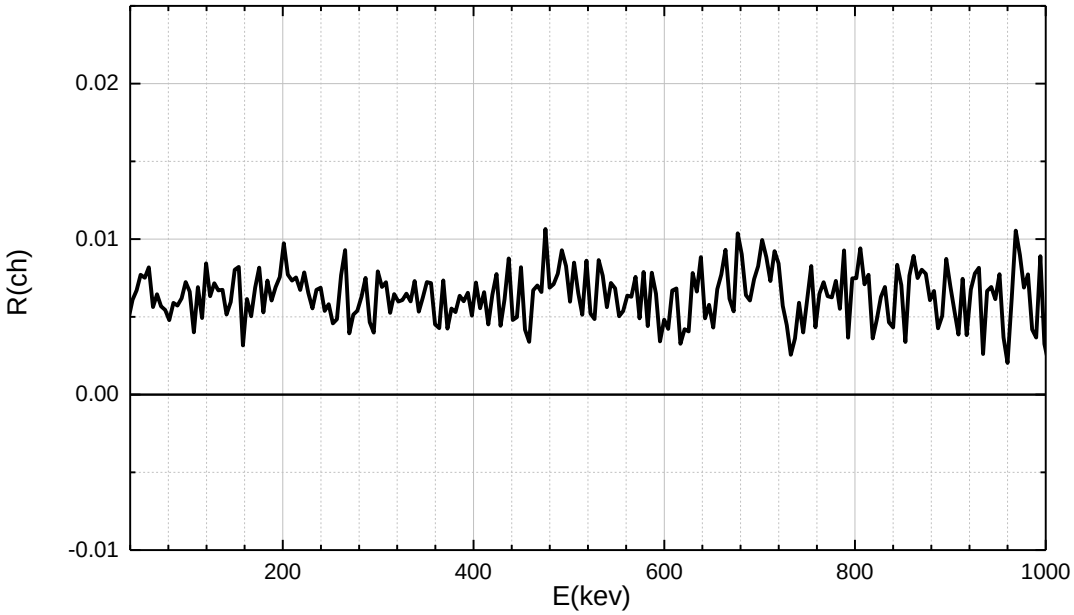

Figure 3- The R(ch) function dependency on the gamma energy emitted from Thorium, after averaging all five results.

Accordingly, for all measured dip events, the average of calculated R(ch) is presented in Fig.3. The averaged R(ch) along the spectra significantly increased due to the increase in neutrino flux emission during the dual cyclotron operation.

Ba-133 system

This study measured Ba-133 for the first time. Six decreases were detected in the total counts following dual cyclotron operations, and the results are listed in Table 3. Fig.4 presents an

example of the detected decrease in Ba-133 total counts on January 4, 2022, 18:00, in response to neutrinos emitted from the two cyclotrons operation on January 4, 2022, at 04:15.

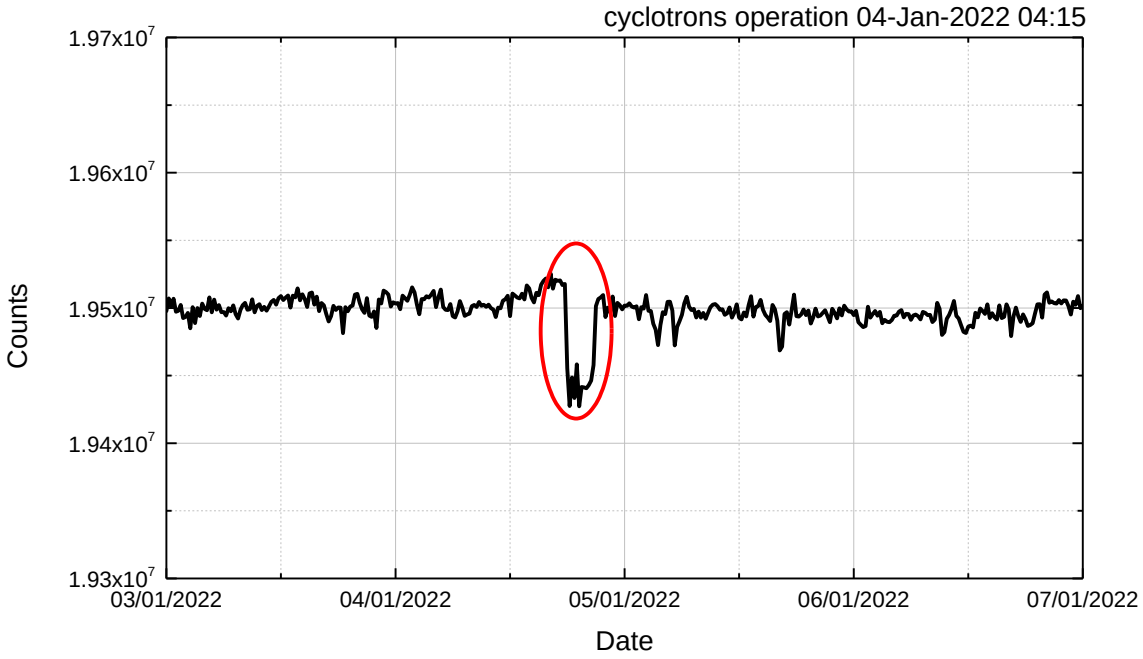

Figure 4- Example of Ba-133 total count mode measurements. Red circles indicate the observed decrease in the counts due to neutrinos emitted from two cyclotrons and interacting with the radio-nuclei.

Table 3 – Summary of the total counts for Ba-133 measurements in response to dual cyclotron operations.

Date of cyclotron operation	Date of sharp dip	cyclotron	Duration (hr)	Current (μA)	Delay (hr)	Count decrease (%)
21-Dec-2021 3:00	21-Dec-2021 18:00	1	0:55	65	15:00	-0.24%
		2	2:50	68		
28-Dec-2021 3:00	28-Dec-2021 18:00	1	4:40	67	15:00	-0.35%
		2	7:00	70		
04-Jan-2022 4:15	04-Jan-2022 18:00	1	2:40	68	13:45	-0.29%
		2	6:00	70		
25-Jan-2022 3:30	25-Jan-2022 18:15	1	2:00	65	14:45	-0.32%
		2	3:00	70		
01-Feb-2022 3:25	02-Feb-2022 6:15	1	2:15	65	26:50	-0.27%
		2	3:10	75		
08-Feb-2022 3:45	08-Feb-2022 18:00	1	3:00	68	14:15	-0.32%
		2	5:00	75		

Based on the data, a calculation of the standard deviation was found to be 0.04% and the 'limit of detection' is 0.08%. Ba-133 has 5 known gamma ray emission lines (81 keV, 276keV, 303 keV, 356 keV, 384 keV[29]), however, because the NaI(Tl) detector has a limited spectral resolution, four peaks cannot be separated, as shown in Fig.5A. The R(ch) function in Fig.5B on the same graph reveals that all parts of the Ba-133 spectrum exhibited a decrease.

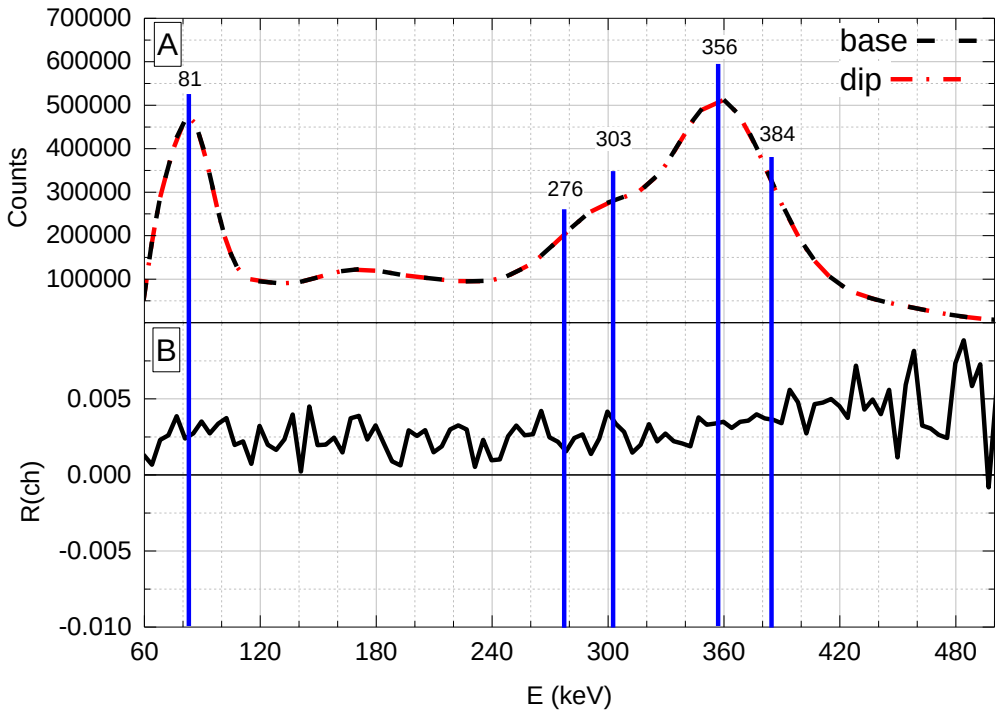

Figure 5- A) The obtained spectrum of Ba-133 after averaging 12 spectra in which the dip occurred (dashed red line) and after averaging 12 spectra of the baseline (black dashed line). B) is the R(ch) calculated for these spectra. The blue vertical lines indicate the gamma energy emission lines of Ba-133.

Due to the NaI(Tl) resolution, the ROI was selected in the area of the 356 keV photopeak. The right and left sides of this peak were tested; on the left side there is also a 384 keV photopeak, and on the right side there are peaks of 303 keV and 276 keV. In addition, the 81 keV photopeak was examined. Table 4 summarizes the R(ch) function for each of the measured spectra in all the ROI channels for photopeaks and the left and right side of the 356 keV photopeak.

Table 4- summary of all ROI in the R(ch) for Ba-133 count rate responses due to dual cyclotron operation (each channel is 4.29 keV).

Date:			21-Dec-21	28-Dec-21	04-Jan-22	25-Jan-22	02-Feb-22	08-Feb-22
E (keV)	Peak Ch	ROI Ch	Ratio Sum					
81	16	12-20	0.028	0.032	0.027	0.033	0.025	0.023
356	81	54-116	0.296	0.193	0.244	0.200	0.294	0.249
left of peak 356		54-81	0.024	0.093	0.076	0.104	0.030	0.067
right of peak 356		81-116	0.275	0.103	0.172	0.099	0.268	0.186

Table 4 reveals that the R(ch) of the right side of the 356 keV peak increased slightly more than the left side of the same peak. This led us to examine separately the left and the right sides of its photopeak in mono-energetic sources.

When averaging the photopeak area ROI for Ba-133, there are also negative values in the R(ch) function. However, for the R(ch) values, as shown in Fig.6, the result clearly demonstrated a decrease in the total observed counts, contributing to a decrease in all parts of the spectrum as well.

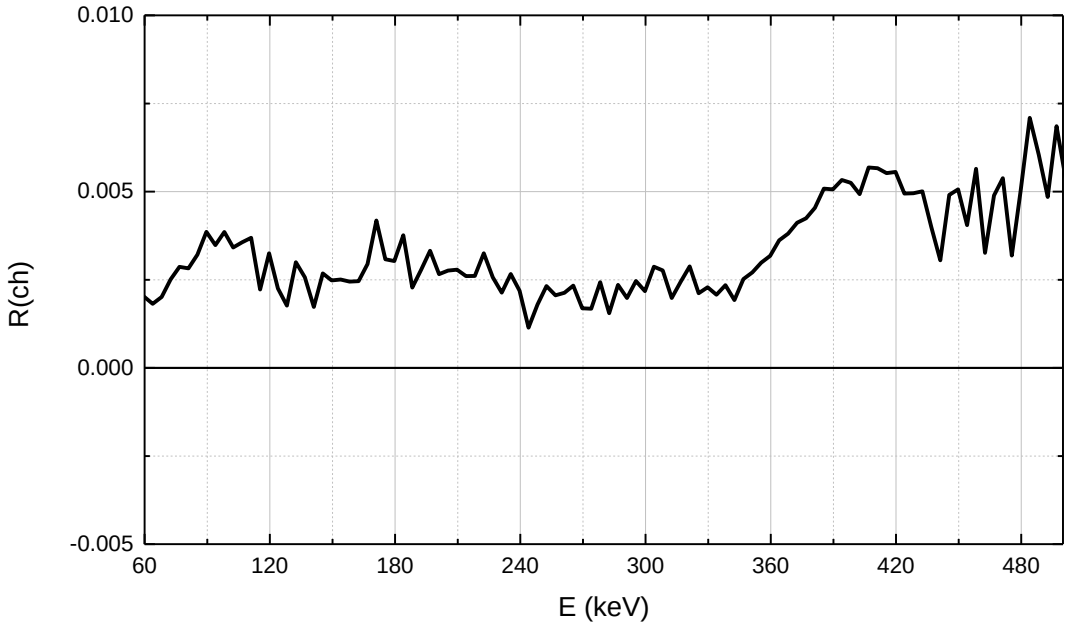

Figure 6- Averaging R(ch) function of Ba-133 for all six results, as a dependence on the gamma energy emitted from the source.

Mn-54 system

Mn-54 is a mono-energetic gamma radiation source with an energy line of 835 keV[29]. In previous studies, Mn-54 was found to respond to solar flares[20,30], and therefore we chose to use Mn-54 as a gamma source in this study.

Six decreases in Mn-54 total counts were detected following dual cyclotron operation, as listed in Table 5. Fig.7 presents an example of the Mn-54 total counts on November 2, 2021, in response to neutrinos emitted from dual cyclotron operation on October 28, 2021.

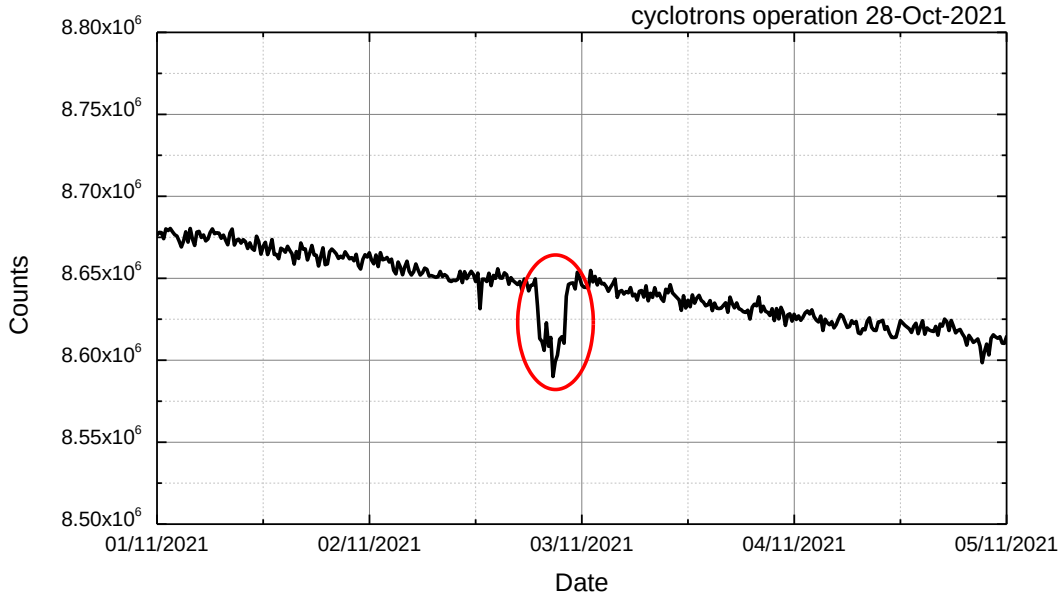

Figure 7- Example of Mn-54 total counts. Red circles indicate the observed decrease in total counts due to the operation of two cyclotrons and interactions with the radio nuclei.

Table 5- Summary of all Mn-54 total count mode responses to cyclotron operations.

Date of cyclotron operation	Date of sharp dip	cyclotron	Duration (hr)	Current (μA)	Delay (days)	Count decrease (%)
07-Oct-2021	12-Oct-2021	1	4:25	65	5	-0.64%
		2	4:00	75		
21-Oct-2021	26-Oct-2021	1	3:20	70	5	-0.40%
		2	3:20	74		
28-Oct-2021	02-Nov-2021	1	2:50	70	5	-0.41%
		2	3:50	67		
04-Nov-2021	09-Nov-2021	1	2:00	67	5	-0.43%
		2	2:00	72		
18-Nov-2021	23-Nov-2021	1	3:00	70	5	-0.45%
		2	3:30	84		
02-Dec-2021	07-Dec-2021	1	1:15	70	5	-0.39%
		2	1:11	75		

Mn-54 total counts demonstrate a downward trend. Data points were averaged on both sides around the dip in the counts, as shown in Fig.7. The average counts of both sides are required to reduce regular fluctuations from readings[21]. Based on the data, the 'limit of detection' was calculated to be 0.283%. Also, Mn-54 spectral results (Fig.8A) encounter similar difficulty in distinguishing the apparent spectral decrease. Therefore, spectral analysis was performed on Mn-54 results, similarly to the Thorium spectral results. The R(ch) function (Eq.1) for Mn-54 was calculated. Representative results for the R(ch) function and the difference of the obtained spectra on November 2, 2021, are shown in Fig.8B.

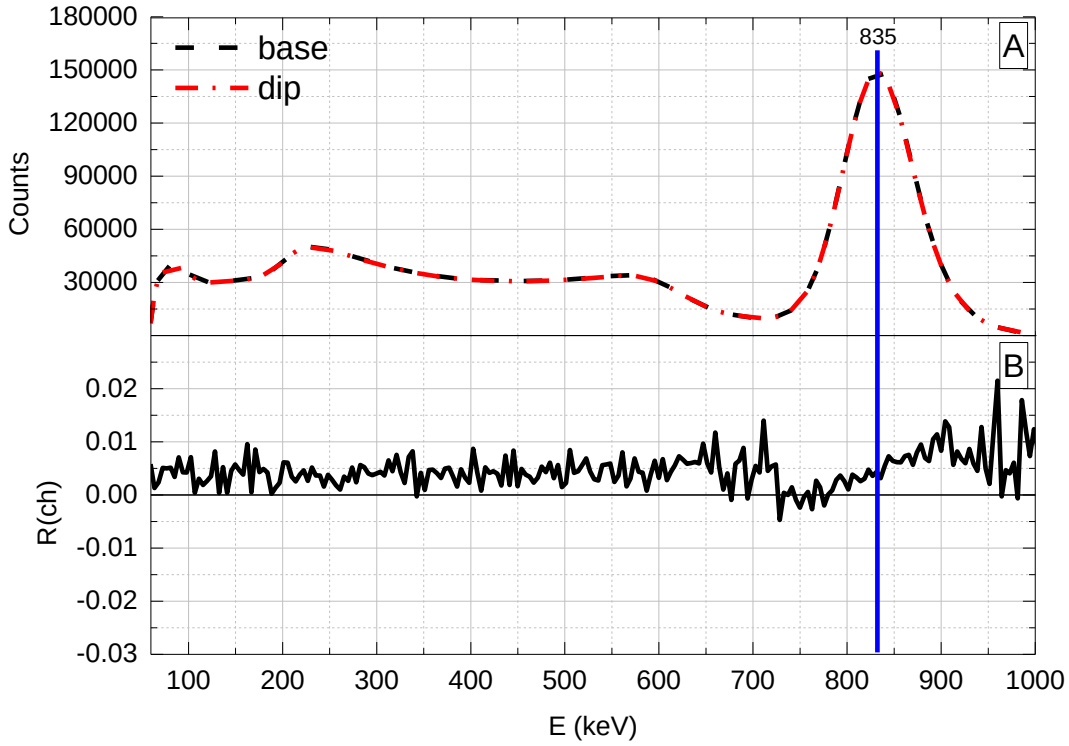

Figure 8- A) Graph showing the obtained spectrum of Mn-54 after averaging 12 spectra in which the dip occurred (dashed red line) and after averaging 12 spectra of the baseline (black dashed line). B) Graph shows the calculated R (ch) for these spectra. The blue vertical line indicates the gamma energy emission line of Mn-54.

As a result of the Mn-54 spectral analysis, we can examine the changes in the photopeak counts area. The peak-to-total counts ratio was obtained: at the base it was 0.4272, and at the dip it was 0.4270. The base ratio and the dip ratio showed a difference within the statistical error of the counts. We performed ROI calculations for the entire photopeak, and in addition we performed ROI calculations for the left and right sides of the photopeak in Fig.8 (Lower graph): a difference around the centroid was indicated. R(ch) function for each dip spectra were totaled for full peak ROI channels and for the left and right sides of the photopeak. The results are summarized in Table 6.

Table 6- Summary of all ROI in the calculated R(ch) function for Mn-54 count responses due to dual cyclotron operation (each channel is 4.29 keV).

Date:			12-Oct-21	26-Oct-21	02-Nov-21	09-Nov-21	23-Nov-21	07-Dec-21
E (keV)	Peak Ch	ROI Ch	Ratio Sum					
835	191	164-216	0.441	0.195	0.242	0.228	0.251	0.243
left side		164-191	0.254	0.152	0.004	0.148	-0.089	0.223
right side		191-216	0.199	0.047	0.201	0.083	0.346	0.022

Examination of the ROI photopeak area in Mn-54 reveals that there is always a positive R(ch), however, only one result presented a negative value of the R(ch) function. When we checked one side of the full peak, differences in R(ch) were detected between the right and the left sides.

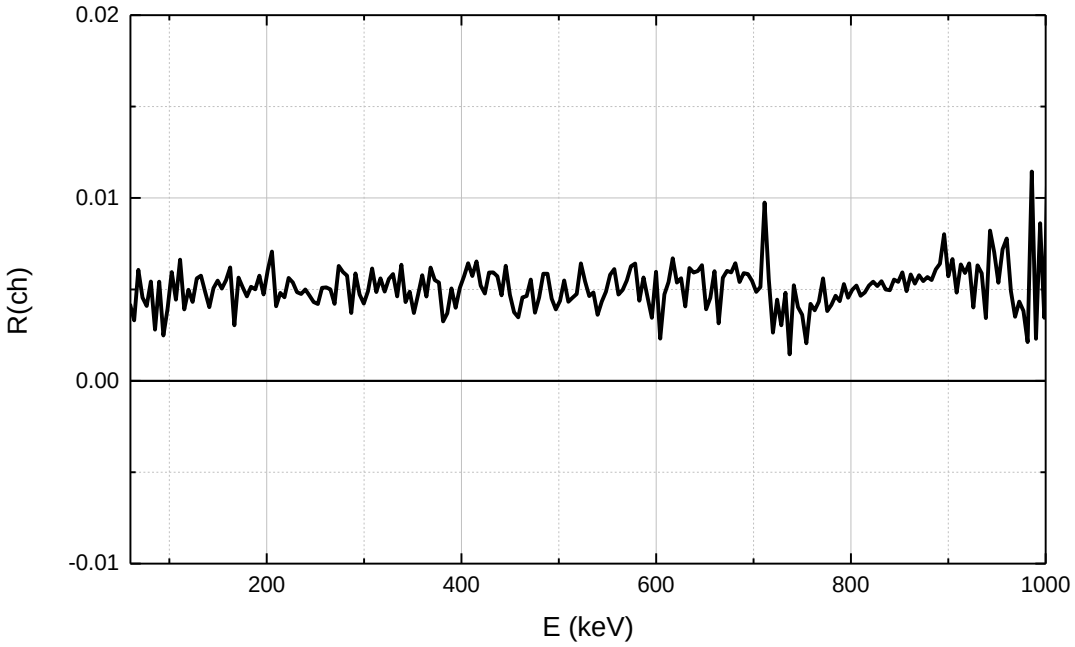

Figure 9- Averaged for all R(ch) function for Mn-54 results

For all measured dip events, the average of calculated R(ch) is presented in Fig.9. The averaged R(ch) along the spectra increased as a result of the increase in neutrino flux emission during dual cyclotron operation. Fig.9 demonstrates that at energies above the

gamma emission line, above 835 keV, the R(ch) significantly increased. This occurred even when the peak centroid did not show any displacement.

Cs-137 system

Changes in the Cs-137 count rate are reported for the first time in this study. The Cs-137 radioisotope is particularly interesting because it is widely used as a calibration source. Six decreases were detected in the total counts for the gamma rays emitted by Cs-137 following dual cyclotron operation, as listed in Table 7. Fig.10 presents an example of a total counts decrease that was measured in Cs-137 on February 15, 2022, in response to neutrinos emitted from the operation of the cyclotrons on February 10, 2022.

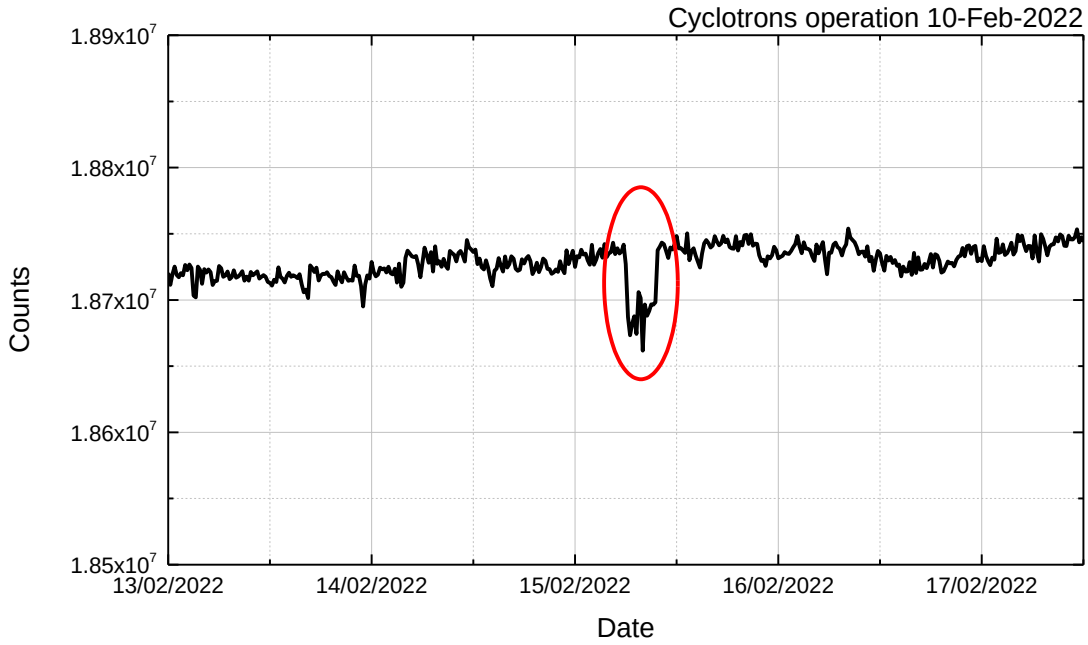

Figure 10 – An example of total count mode for Cs-137. The red circle marks a dip resulting from interactions with neutrinos emitted from two cyclotrons operated simultaneously.

Table 7 – Summary of all Cs-137 total count rate responses due to dual cyclotron operation.

Date of cyclotron operation	Date of sharp dip	cyclotron	Duration (hr)	Current (μA)	Delay (days)	Count decrease (%)
10-Feb-2022	15-Feb-2022	1	3:00	70	5	0.27%
		2	6:00	74		
17-Mar-2022	23-Mar-2022	1	2:40	67	6	0.27%
		2	3:10	73		
24-Mar-2022	29-Mar-2022	1	4:25	74	5	0.29%
		2	6:20	74		
31-Mar-2022	05-Apr-2022	1	2:50	70	5	0.25%
		2	2:00	73		
14-Apr-2022	19-Apr-2022	1	3:30	65	5	0.27%
		2	3:40	71		
19-Apr-2022	26-Apr-2022	1	2:55	65	7	0.34%
		2	5:45	72		

The standard deviation of the measured decrease was found to be 0.04%, and the ‘limit of detection’ is 0.10%. Similarly, analysis was performed for Cs-137 results, in the same fashion

as the Thorium results were analyzed. R(ch) function for Cs-137 was calculated. Representative results for the R(ch) function and the difference in the obtained spectra on February 15, 2022, are shown in Fig.11.

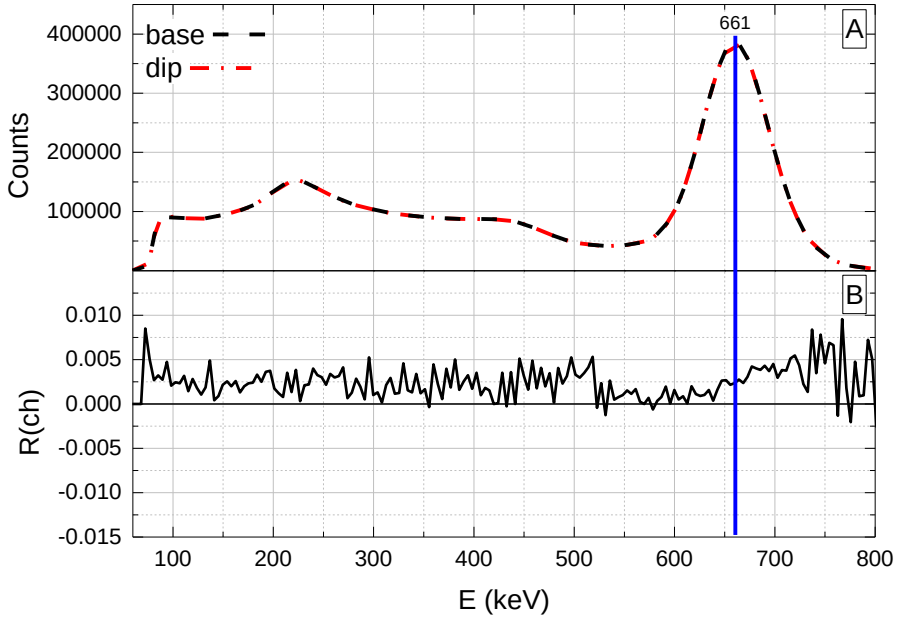

Figure 11 – A) The upper graph shows the spectra obtained for Thorium after averaging 12 spectra at the time when the dip occurred (dashed red line) and after averaging 12 spectra of the baseline before the dip occurred (black dashed line). The blue vertical line shows the gamma energy emission line of Cs-137. B) Is the change using the R(ch) function that was calculated for these spectra.

The Cs-137 photopeak occurs at an energy of 662 keV[29]. The peak-to-total counts ratio was obtained: at the base it was 0.4705, and at the dip it was 0.4704. The base ratio and the dip ratio showed a difference within the statistical error of the counts.

We performed an ROI calculation for the single photopeak, and for its left and right sides. R(ch) function for all spectra was performed for all the ROI channels of the photopeak, as presented in Table 8.

Table 8 –Summary of the ROI in the R(ch) of the obtained six dips in table 7, each channel is 4.29 keV

Date:			15-Feb-22	23-Mar-22	29-Mar-22	05-Apr-22	19-Apr-22	26-Apr-22
E (keV)	Peak Ch	ROI Ch	Ratio Sum					
661	145	122-178	0.151	0.062	0.389	0.243	0.126	0.258
left to peak		122-145	0.027	-0.041	-0.067	-0.015	0.099	0.020
right to peak		145-178	0.126	0.104	0.457	0.260	0.031	0.242

After investigating the ROI of the photopeak area in Cs-137, we found that there are also negative values in the R(ch) function. However, the R(ch) values results, as shown in Fig.12, clearly demonstrate that a decrease in the total observed counts caused a decrease in the overall spectrum as well.

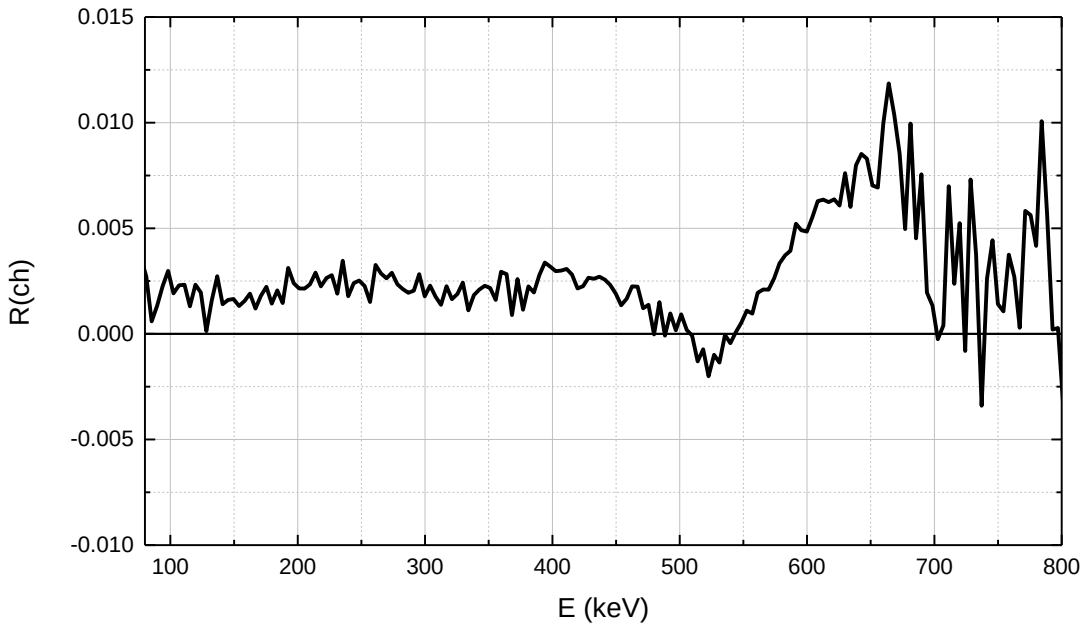

Figure 12 – The R(ch) function dependency on the gamma energy emitted from Cs-137, after averaging all six results.

In the natural Thorium results, a delay of nine days between dual cyclotron operation and the decrease in the spectra we found in the spectral measurement. The results regarding Thorium confirm our previous findings, which were recorded using a total-count gamma radiation detector[21].

Ba-133 was found to have a delay response of about 15 hours from the dual cyclotron operation event until a decrease in the detected count rate. Cs-137 was found to have a delay response of about five days from dual cyclotron operation until a decrease in the gamma counts was detected.

Spectral measurements for Thorium, Mn-54, Ba-133 and Cs-137 sources showed decreases through photopeak and Compton scattering counts that are affected by changes in the neutrino flux.

Photofraction (Peak to total) is the ratio of the area under the photopeak to the area under the entire response. The calculation for our measurements was obtained using the same photofraction ratio as Synder`s experiments[31]. The photofraction ratio remained unchanged along the decreased spectra. It is important to note that if a change was found in the Compton only, this might be cause for concern, suggesting that there is a problem with the detector itself. For example, neutrons entering the detector and reacting with the iodine in NaI(Tl)[32].

The spectral results for the two mono-energetic radioisotopes presented differences between the right and left sides of the photopeak (see Fig. 9 and Fig. 12). This difference might be explained similarly to XRF spectral peak splitting, due to spin-orbit interaction[34].

In this study, neutrino interaction with the radionuclide is evident. Neutrinos have a spin ½ and therefore might magnetically interact with the nucleus, in analogy to neutron magnetic scattering with the nuclei spin in lattice. Similarly to neutrons that can scatter by spin-orbital, or by spin-spin interactions, it might be assumed that neutrinos interact in a similar manner and show diffraction patterns[35-36].

Gamma spectra decrease as a result of changes in neutrino flux indicates that the radioactive decay processes in Thorium, Ba-133, Mn-54, and Cs-137 can change and temporarily slow down.

Conclusions

Our previous research established a new method for measuring changes in counts of gamma-emitting materials caused by varying fluxes of neutrinos emitted by solar flares or cyclotrons. These measurements were recorded using NaI(Tl) signal channel gamma radiation detectors. NaI(Tl) spectral measurements with data analysis were recorded using an MCA for Th-232 and Mn-54 to verify the reliability of count decreases previously obtained. Spectral analysis enables us to indicate any possible malfunctions, such as HV bias instability, by assuring the absence of deviations in the spectral shape and repeatability. Repeated measurements every 15 minutes demonstrated recurrence of the spectrum, without photopeak centroid shifts. This confirms that the NaI(Tl) measurement method is a reliable technique for measuring changes in gamma radiation decay rates, and the decreases found are not due to detector instability. Furthermore, it was found for the first time that the gamma radiation emitted by Ba-133 and Cs-137 is also affected by changes in neutrino flux.

The count rate decrease found in this study indicates that gamma emission reduction occurred in the examined radio-nucleus, hence the momentum selection rules of the transition between two nuclear levels possibly altered. The neutrino presumably interacts magnetically with the nucleus spin, and in so doing influences the momentum selection rules of the gamma emission multipolarity.

The use of gamma emitters to detect neutrinos yields advantageous results compared with the complex existing detectors. Indeed, radioactive materials have a constant level of background counts, preventing underground measurements using highly sensitive detectors.

References

[1] Nakazato K., et al., Observing Supernova Neutrino Light Curves with Super-Kamiokande. II. Impact of the Nuclear Equation of State, The Astrophysical Journal, V.925, 2022. http://dx.doi.org/10.3847/1538-4357/ac3ae2.

[2] Duffy K. E., et al., Neutrino interaction measurements with the MicroBooNE and ArgoNeuT liquid argon time projection chambers, The European Physical Journal Special Topics, 2022, https://doi.org/10.1140/epjs/s11734-021-00297-5.

[3] Orekhov V. and Wurm M., Development of the comprehensive analysis tools for the Supernova neutrino detectors. Il nuovo cimento C, V.45 (1), pp:1-5, 2022.

[4] Lutostansky Y.S., et al., New prospects for iodine detector and Solar neutrinos registration, Physics Letters B, V.826, 2022, https://doi.org/10.1016/j.physletb.2022.136905.

[5] Netrakanti P.K., et al., Measurements using a prototype array of plastic scintillator bars for reactor based electron anti-neutrino detection, Nuclear Instruments and Methods in Physics Research Section A, V.1024, 2022, https://doi.org/10.1016/j.nima.2021.166126.

[6] McKinsey D.N., Coakley K.J., Neutrino detection with CLEAN, Astroparticle Physics, V. 22 (5-6), pp: 355-368, 2005, https://doi.org/10.1016/j.astropartphys.2004.10.003.

[7] Scholberg K., Supernova Neutrino Detection, Annual Review of Nuclear and Particle Science, V.62, pp:81-103, 2012. https://www.annualreviews.org/doi/abs/10.1146/annurev-nucl-102711-095006

[8] Kodama K. et al., Final tau-neutrino results from the DONuTexperiment, Physical Review D, V.78 (5), pp: 052002-1-20, 2008.

[9] Aartsen M. G. et al., Measurement of the multi-TeV neutrino interaction cross-section with IceCube using Earth absorption, Nature, V.551, pp:596-600, 2017

[10] Goncharov M. et al., Precise Measurement of Dimuon Production Cross-Sections in ν_μ Fe and $\bar{\nu}_\mu$Fe Deep Inelastic Scattering at the Tevatron, FERMILAB-Pub-01/034-E, March 2002.

[11] Stein R. et al., A tidal disruption event coincident with a high-energy neutrino, Nature Astronomy, V.5, pp: 510-518, 2021.

[12] Abreu H. et al., First neutrino interaction candidates at the LHC, UCI-TR-2021-04, KYUSHU-RCAPP-2020-04, CERN-EP-2021-087

[13] Halzen F., Kheirandish A., Black holes associated with cosmic neutrino flares, Nature Physics, V.16 (5), pp:498-500, 2020.

[14] Aprile E. et al., Observation of two-neutrino double electron capture in 124Xe with XENON1T, Nature, V.568 (7753), pp:532-535, 2019.

[15] Davis R., A review of measurements of the solar neutrino flux and their variation,Nuclear Physics B – Proceedings Supplements, V48 (1–3), pp: 284-298, 1996. https://doi.org/10.1016/0920-5632(96)00263-0.

[16] Ryazhskaya O.G., Volkova L.V., Zatsepin G.T., "Neutrinos From Solar Flares at the Earth" Nuclear Physics B Proceedings Supplements, V.110, pp:358-360, 2002.

[17] Walg J., Rodnianski A. and Orion I., "Evidence of Neutrino Flux effect on Alpha Emission Radioactive Half-Life", ATINER's Conference Paper Proceedings Series PHY2019-0137 Athens, 7 August 2019.

[18] Walg J., Rodnianski A., Orion I., "Solar Flare Detection Method Using Rn-222 Radioactive Source", GSC Advanced Research and Reviews, V.05(02), pp:159–166, 2020.

[19] Peleg Y., Walg J. and Orion I., Solar Flare Effect on Geological Thorium Radiometric Dating, Aspects in Mining & Mineral Science, V.7(1), pp:772-776, 2021.

[20] Walg J., Peleg Y., Rodnianski A., Hazenshprung N., Orion I., Effect of Solar Flares nn ^{54}Mn and ^{57}Co Radioactive Decay Constants Performance, Nuclear Technology & Radiation Protection, V36(3), Pp: 219-223, 2021.

[21] Walg J., Feldman J., Peleg Y., Azarzar A., Mishani E. and Orion I., Neutrino Effect on Gamma Radiation Emission from Radioactive Nuclides, EasyChair Preprints, Preprint 7517 (2022-02-27).

[22] Knoll, G. F. Radiation Detection and Measurement, 3rd ed. Chapters 3 & 8 &9 (John Wiley and Sons 2000).

[23] Walg J., Feldman J., Izarzar A., Rodinianski A., Mishani E. & Orion I., Cyclotron-produced neutrons measurements using Chlorine activation, Nuclear Inst. and Methods in Physics Research B 503, 1-5, 2021.

[24] Wielopolsky L. and Shreeve W., Instrumentation for Body Composition Analysis Present and Future (page 20), in Workshop on Body Composition in Basic and Clinical Research and The Emerging Technologies December 14th , 2000, Brookhaven National Laboratory, Upton, NY 11973 (Formal Report BNL-52630).

[25] Tsoulfanidis, N., & Landsberger, S. (2015). Measurement and Detection of Radiation (4th ed.). CRC Press (chapter 9). https://doi.org/10.1201/b18203.

[26] Charitonidis N., Longhin A., Pari M., Parozzi E.G., Terranova F., Design and Diagnostics of High-Precision Accelerator Neutrino Beams. Appl. Sci., V11(4),2021. https://doi.org/10.3390/app11041644.

[27] Alsharo'a M. M., et al., Recent progress in neutrino factory and muon collider research within the Muon Collaboration, Phys. Rev. ST Accel. Beams, V6 (8), 2003. https://link.aps.org/doi/10.1103/PhysRevSTAB.6.081001.

[28] Kube G., T Particle beam diagnostics and control, Conference Proceedings, 2012.

[29] Chu S.Y.F., Ekström L.P. and Firestone R.B., The Lund/LBNL Nuclear Data Search Version 2.0, February 1999. http://nucleardata.nuclear.lu.se/toi/index.asp.

[30] Jenkins, J. H., Fischbach, E., Perturbation of Nuclear Decay Rates During the Solar Flare of 2006 December 13, Astroparticle Pysics, 31 (2009), 6, pp. 407-411.

[31] Snyder B. J., Nucl. Instr. and Meth. 46 (1967) 173.

[32] Gardner R. P et al., NaI detector neutron activation spectra for PGNAA applications, Applied Radiation and Isotopes, V53(4–5), pp:483-497, 2000. https://doi.org/10.1016/S0969-8043(00)00198-6.

[34] Hollas J. M., Modern Spectroscopy, 4th ed., John Wiley & Sons (2003).

[35] White R. M., Quantum Theory of Magnetism Magnetic Properties of Materials, 3rd ed. Chapter 10, Springer-Verlag Berlin Heidelberg (2007).

[36] Sarenac D. et al., Generation and detection of spin-orbit coupled neutron beams. Proc Natl Acad Sci U S A. 2019 Oct 8;116(41):20328-20332. doi: 10.1073/pnas.1906861116. Epub 2019 Sep 23. PMID: 31548384; PMCID: PMC6789912.